Available online at www.sciencedirect.com
SCIENCE DIRECT®
Journal of Solid State Chemistry 179 (2006) 91–95
JOURNAL OF SOLID STATE CHEMISTRY
www.elsevier.com/locate/jssc

Synthesis of nickel nanoparticles and carbon encapsulated nickel nanoparticles supported on carbon nanotubes

Jipeng Cheng[a,*], Xiaobin Zhang[a], Ying Ye[b]

[a]Department of Materials Science and Engineering, Zhejiang University, Hangzhou 310027, PR China
[b]Department of Earth Science, Zhejiang University, Hangzhou 310027, PR China

Received 3 August 2005; received in revised form 30 September 2005; accepted 3 October 2005
Available online 2 November 2005

Abstract

Nickel nanoparticles were prepared and uniformly supported on multi-walled carbon nanotubes (MWCNTs) by reduction route with CNTs as a reducing agent at 600 °C. As-prepared nickel nanoparticles were single crystalline with a face-center-cubic phase and a size distribution ranging from 10 to 50 nm, and they were characterized by transmission electron microscopy (TEM), high-resolution TEM and X-ray diffraction (XRD). These nickel nanoparticles would be coated with graphene layers, when they were exposed to acetylene at 600 °C. The coercivity values of nickel nanoparticles were superior to that of bulk nickel at room temperature.

Keywords: Carbon nanotube; Nickel nanoparticles; Microstructure; Carbon encapsulation; Magnetic property

1. Introduction

Carbon materials are often used as support for preparing metal-based catalyst due to resistance to acid/basic media and easy recovery of precious metals by support burning [1]. Carbon can present many allotropic forms, which includes fullerenes [2] and carbon nanotubes (CNTs) [3] that were discovered decades ago. Recently, CNTs have generated an intense effervescency in scientific community. The preparation of nanocomposite materials from CNTs and metal or metal oxide nanoparticles has important implications to the development of advanced catalyst and sensory materials. This category of composite currently attracted much attention [4]. The modification and anchoring of nanoparticles on the external surface of CNTs can dramatically influence their physical properties, such as electrical conductance, which may lead to novel changes that are relevant to practical applications. Kong et al. [5] reported that modification of CNTs with Pd particles would impact sensitivity of nanotube electrical properties to fabricate sensors. Various metal and metal oxide nanoparticles loaded on CNTs were reported recently, such as Pt [6], Cu_2O [7], Au [8], TiO_2 [9], CeO_2 [10].

Metallic nickel nanoparticles have attracted much attention because of their applications as catalyst and conducting or magnetic materials [11–12]. It is anticipated that nanoscaled nickel particles should be of unusually catalytic ability and differ considerably from that of bulk materials. While the nanoscaled aspects usually cause an intractable agglomeration, it will constrain the potential merit to certain degree. So, CNT is an ideal support for nickel nanoclusters because of its nanoscaled and steady structure characteristics and morphology, as well as inert and resistant properties.

Metal nanoparticles are usually activated and tend to be oxidized in the open air. Carbon encapsulation of magnetic nanoparticles could retain their intrinsic nanocrystalline properties [13] and keep them from oxidization [14]. The carbon coatings can endow these magnetic particles with biocompatibility and stability in many organic and inorganic media. Those magnetic systems are suitable for potential applications like ferrofluids, magnetic recording media, and medical imaging. Some novel magnetic systems of carbon encapsulated ferromagnetic materials, e.g., iron, cobalt and nickel, have successfully been obtained by a

*Corresponding author. Fax: +86 571 87951411.
E-mail address: mseem@zju.edu.cn (J. Cheng).

0022-4596/$ - see front matter © 2005 Elsevier Inc. All rights reserved.
doi:10.1016/j.jssc.2005.10.001

number of researchers [13,15–16]. However, the preparation of carbon encapsulated metallic nanoparticles in a high yield with a simple method still represents a significant challenge [14,17–18].

In this paper, a simple method is described for the preparation of nickel nanoparticles well dispersed on multi-walled CNTs (MWCNTs). The resultant hybrid is characterized in detail and applied to react with acetylene at 600 °C. These metallic nanoparticles are thus encapsulated with graphene sheets. The encapsulation procedure is based on the large body of knowledge developed for the growth of CNTs. The magnetic properties of as-prepared nickel nanoparticles are preliminary evaluated.

2. Experimental section

The CNTs used as the support of nickel particles were fabricated by pyrolysis of acetylene using metals supported on nanocrystalline $CaCO_3$ [19]. Fe–Co bimetallic catalyst dispersed on $CaCO_3$ reacted with acetylene at 750 °C to obtain CNTs. As-prepared CNTs were purified by refluxing in diluted nitric acid for hours to remove residual impurities at 140 °C. After cooling to ambient temperature, the black suspension was filtered with a ceramic filter and washed with adequate distilled water until neutral, and then dried. Some CNTs (~1 g) were thoroughly dispersed into a saturated $Ni(NO_3)_2$ solution (~30 ml) for two days at room temperature. After filtration with filter paper, the nickel-impregnated CNT powder was dried at 130 °C.

The nickel-impregnated CNTs were kept at 600 °C for 20 min under nitrogen atmosphere. Then, nickel ions on CNTs were reduced by its support and transformed into nanoclusters, which was confirmed by micrometric analyses. A hybrid of nickel-deposited CNTs was thus obtained. To encapsulate these nickel particles, an amount of nickel-deposited CNTs was applied as catalyst to decompose acetylene at 600 °C, which is based on the CNT synthesis. These nickel nanoparticles were thus fully encapsulated by graphene layers.

Transmission electron microscopy (TEM) was used to observe the nanostructures of CNTs and nickel nanoparticles. X-ray diffraction (XRD) spectra were recorded with D/max-rA using Cu$K\alpha$ radiation. Field emission scanning electron microscopy (FSEM, FEI sirion) equipped with an energy dispersive X-ray spectrometer (EDS) was employed for morphology examination and elemental analysis. Finally, the magnetic properties of products were obtained from hysteresis loops recorded in a vibrating sample magnetometer (VSM) at room temperature.

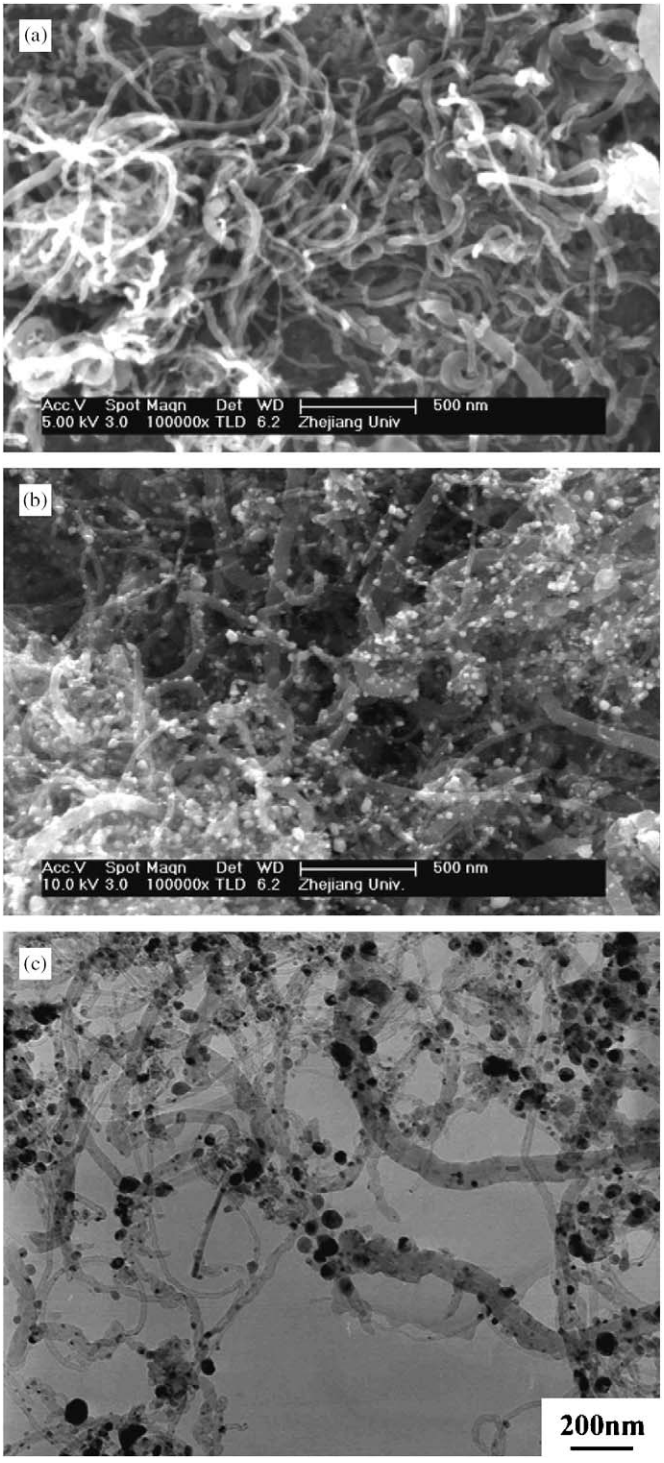

Fig. 1. SEM image of purified MWCNTs (a), SEM (b) and TEM (c) images of nickel particle deposited CNTs.

3. Results and discussion

Figs. 1a and b show two typical SEM micrographs of MWCNTs purified by nitric acid and nickel-deposited carbon tubes, respectively. From Fig. 1a, it can be seen that the purified CNTs are bare multi-wall with a large diameter distribution. However, after the deposition of nickel, a number of nanoparticles homogeneously attached on the external surface of CNTs were observed with a wide size distribution, as shown in Fig. 1b. Fig. 1c shows a bright-field TEM image of nickel particles attached on CNTs with a high magnification. The morphologies of particles and CNTs are clearly observed. The size of nanoparticles varies from 10 to 50 nm. Most particles are quasi-spherical in

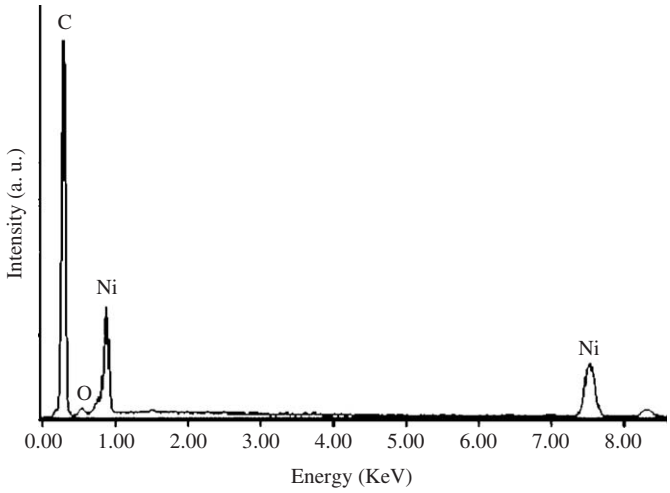

Fig. 2. EDS spectrum of nickel-deposited carbon nanotubes.

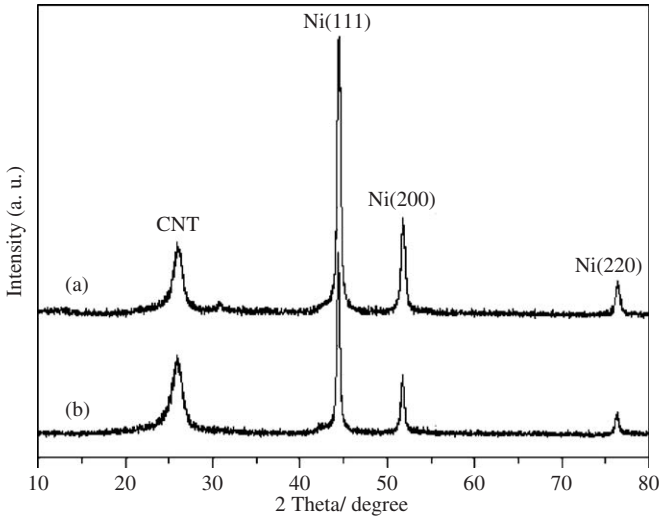

Fig. 3. XRD patterns of nickel-deposited CNTs (a) and carbon encapsulated nickel particles (b), showing the diffraction peaks of graphite and nickel.

shape and tightly dispersed on the surface of CNTs. The elemental analysis by EDS proves that the resulting product contains the elements C, nickel, and O in Fig. 2. The results of EDS indicate that the content of nickel in the compound is about 12% in weight. Combining these with SEM and TEM analyses, it is reasonable to conclude that nickel nanoparticles have been successfully prepared on CNTs surface. The presence of oxygen comes from some functional groups that were introduced by nitric acid oxidation [20]. However, few nickel nanoparticles could be attached to the as-prepared CNTs by the same procedure.

The inert, pristine surface of as-prepared CNTs makes it difficult for attachment of metal precursors [21]. It has been pointed out that most metals would not adhere to them [22]. Then, two main approaches are developed, i.e. surface modification and sensitization activation. The former is associated with the oxidation of the nanotube surface to create functional groups and increase metal nucleation [8,21]. The latter consists of the generation of small nuclei to further promote metal deposits on CNTs [23]. The reasonable formation process of nickel nanoparticles in our case is as following. In reflux with nitric acid, the surface graphene layers of CNTs would react with the oxidants and produce a high density of various functional groups, such as hydroxyl, carboxyl and carbonyl [20]. With the presence of high-density surface functional groups, CNTs showed much better dispersibility in water compared with the raw nanotube material [21]. These functional groups could provide active sites for interaction with nickel cations during the immersion process. At elevated temperature, nickel ions congregated on the surface of CNTs and were reduced by carbon atoms in the inert atmosphere at 600 °C. Hence, nickel nanoparticles were formed on CNTs. The method to deposit nickel nanoparticles on CNTs is easily carried out in our case, avoiding sensitization and activation [23], as well as hydrogen reduction [7].

The powder XRD profile of nickel-deposited CNTs (Fig. 3a) clearly shows the presence of a majority of face-centered-cubic (fcc) nickel (PCPD file: No. 04-0850), with an individual diffraction peak of graphite (002) at ~26° from CNTs. In addition, there is no nickel carbide of the cementite phase and nickel oxides detected. In accordance with above results, one can believe that nickel ions originally absorbed on CNTs are reduced by carbon atoms and they agglomerate to form nanoparticles. Koltypin et al. [24] have also found that nickel ions could be reduced to nanosized nickel particles with amorphous carbon as reducing agent in an inert gas atmosphere at 500 °C. Even micron-sized nickel oxide particles could be reduced by natural graphite at 950 °C [25]. The broadening of nickel peaks in the XRD pattern is due to the small particle size. The size of the nickel nanoparticles is also estimated using the Scherer equation in a form: $t = 0.9\lambda/B\cos\theta_B$ [26], where t is the particle size, λ the characteristic wavelength of the X-ray used, B the angular width in radians at an intensity equals to half of the maximum peak intensity, and θ_B the Bragg angle in degree at which the diffraction occurs. The average particle size of the deposited nickel nanoparticles is estimated as 19 nm, calculated from the Scherer equation using nickel (111) peak at 2θ of 44.5°. This size generally approximates to that of TEM observations.

A magnified view of a nickel particle is presented in Fig. 4, a typical high-resolution TEM micrography. It displays fringe patterns, indicating the crystalline nature of these nickel particles. Nickel nanoparticles dispersed on the CNTs are all single crystalline. Fig. 4 represents such a nickel particle. Viewed along the [011] direction, two twin planes are detected with lattice spacing around 0.2 nm, which corresponds to the 1 1 1 plane, i.e. (11−1) and (1−11) planes (marked). These planes enclose an angle of

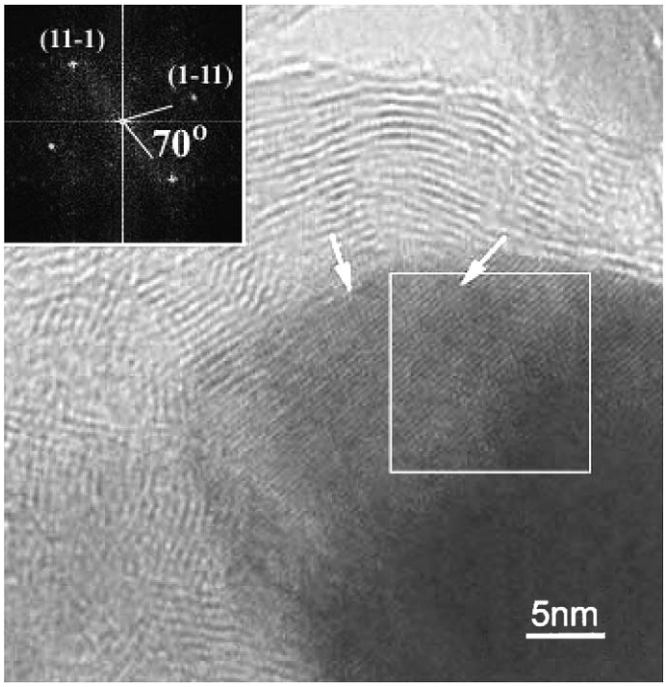

Fig. 4. HRTEM micrograph of a nickel nanoparticle, evidencing its crystalline structure. Twin (111) planes are indicated with arrows. Inset is a Fourier transform image of the marked area.

70.3°, which are consistent with standard fcc nickel crystal. Fast Fourier transform (FFT) from the marked square region in the high resolution TEM image of the nickel nanoparticle shows spots corresponding to the (111) planes of nickel, as presented in the inset of Fig. 4.

After as-prepared nickel-CNT hybrid reacted with acetylene at 600 °C for 20 min, most nickel nanoparticles were wrapped by graphene layer, which was proved by TEM examinations. A TEM picture of the product is shown in Fig. 5. The metallic core is encapsulated in polyhedral concentric graphene shells with a varying number of layers. The XRD pattern of carbon encapsulated nickel particles is presented in Fig. 3b, where only carbon and nickel are detected. Although it is known that nickel is easily oxidized to oxides, some possible oxides such as NiO, Ni_2O_3 are not observed in the XRD profile. This is chiefly due to the encapsulation of graphene layers which protect it from oxidization. Because the sample had been exposed to the air for a long time before being examined, the absence of nickel oxides also confirmed the protection of a closed carbon shell on the material from oxidation by the air, as reported elsewhere [14]. The average metallic particle size of encapsulated nickel is appreciably larger than that of bare nickel particles from the half angular width in their XRD profiles. This results from a sintering propensity at an elevated temperature. Since the catalytic nickel particles have to expose certain surface areas to decompose acetylene in order to obtain carbon atoms, it takes some time for nickel particles to be supersaturated in carbon at such a relatively low temperature. As a result, the thicker graphene layers tend to be accumulated on the surface of the catalytic particles [27]. No carbide peaks in XRD have been exhibited, indicating that excess carbon atoms could not be stabilized as carbide within the particles. These particles are energetically favored for encapsulating themselves into carbon cages that is highly dependent on the experimental conditions, as well as properties of metallic particles.

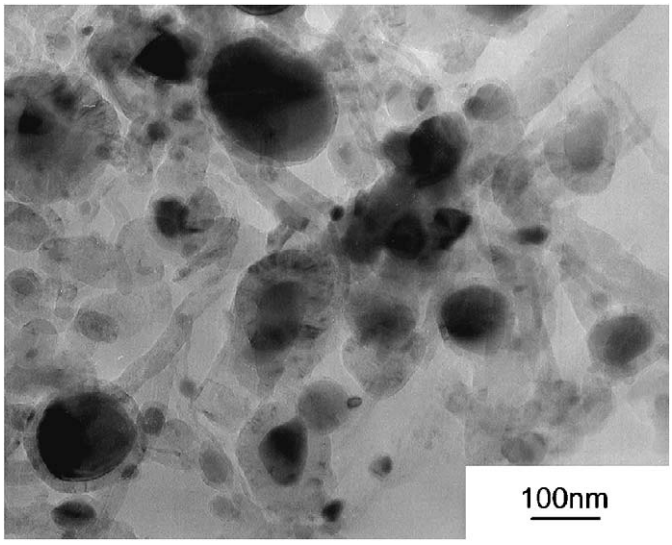

Fig. 5. TEM image of carbon encapsulated nickel nanoparticles that originally deposited on CNTs.

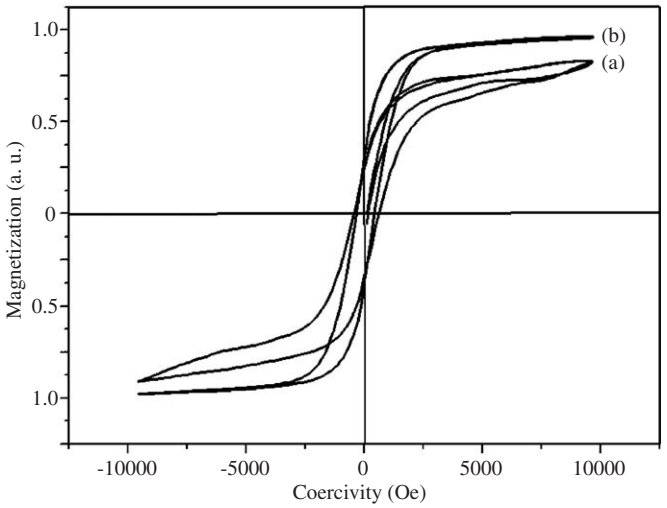

Fig. 6. Room temperature magnetization loops of nickel nanoparticles (a) and carbon encapsulated nickel nanoparticles (b) on CNTs.

The magnetization curves of nickel and carbon encapsulated nickel nanoparticles on CNTs are shown in Fig. 6. The spectra show a ferromagnetic response for two samples and the curves are symmetric around $H = 0$. Its coercivity (H_c) is determined to 525 Oe for nickel nanoparticles, and 384 Oe for carbon encapsulated nickel particles. The H_c value of the bulk nickel is about 100 Oe [16]. The observed increase of H_c with the decreasing of the particles size

correlates well with the fact that the mean particle size approaches the critical size for a single-domain behavior.

4. Conclusions

A facile method for the synthesis of nickel nanoparticle supported on CNTs was described. The oxidation of the CNTs by nitric acid caused its surface accessible to nickel ions that would be reduced by CNTs at elevated temperature under an inert atmosphere, avoiding hydrogen reduction. Nanosized nickel metallic particles with single crystalline nature thus formed on CNTs surface. Carbon encapsulating metal particles was based on the large body of knowledge developed for the growth of CNTs, which was found to be very effective and easily carried out. Our data showed that the coercive field H_c of nickel nanoparticles was several times larger than that of bulk nickel.

Acknowledgments

The authors gratefully acknowledge National Natural Science Foundation of China (No. 50571087) and the Special Funds for Major States Basic Research Project (No.TG20000264-06) of MOST, China.

References

[1] E. Auer, A. Freund, J. Pietsch, T. Tacke, Appl. Catal. A 173 (1998) 259.
[2] H.W. Kroto, J.R. Heath, S.C.O. Brien, R.F. Curl, R.E. Smalley, Nature 318 (1985) 162.
[3] S. Iijima, Nature 354 (1991) 56.
[4] B. Xue, P. Chen, Q. Hong, J. Lin, K.L. Tan, J. Mater. Chem. 11 (2001) 2378.
[5] J. Kong, M.G. Chapline, H.J. Dai, Adv. Mater. 13 (2001) 1384.
[6] T. Matsumoto, T. Komatsu, K. Arai, T. Yamazaki, M. Kijima, H. Shimizu, Y. Takasawa, J. Nakamura, Chem. Comm. 7 (2004) 840.
[7] Y. Yu, L.L. Ma, W.Y. Huang, J.L. Li, P.K. Wong, J.C. Yu, J. Solid State Chem. 178 (2005) 1488.
[8] L.Q. Jiang, L. Gao, Carbon 41 (2003) 2923.
[9] X. Li, J. Niu, J. Zhang, H. Li, Z. Liu, J. Phys. Chem. B 107 (2003) 2453.
[10] Y.H. Li, J. Ding, J.F. Chen, C.L. Xu, B.Q. Wei, J. Liang, D.H. Wu, Mater. Res. Bull. 37 (2002) 313.
[11] M. Yoon, Y. Kim, Y.M. Kim, V. Volkov, H.J. Song, Y.J. Park, I.W. Park, Mater. Chem. Phys. 91 (2005) 104.
[12] Y. Matsumura, K. Tanaka, N. Tode, T. Yazawa, M. Haruta, J. Mol. Catal. A: Chem. 152 (2000) 157.
[13] V.P. Dravid, J.J. Host, M.H. Teng, D. Elliott, J. Hwang, D.L. Johnson, T.O. Mason, J.R. Weertman, Nature 374 (1995) 602.
[14] J.P. Cheng, X.B. Zhang, F. Liu, J.P. Tu, Y. Ye, Y.J. Ji, C.P. Chen, Carbon 41 (2003) 1965.
[15] R. Seshadri, R. Sen, G.N. Subbanna, K.R. Kannan, C.N.R. Rao, Chem. Phys. Lett. 231 (1994) 308.
[16] X.C. Sun, X.L. Dong, Mater. Res. Bull. 37 (2002) 991.
[17] S.W. Liu, J.J. Zhu, Y. Mastai, I. Felner, A. Gedanken, Chem. Mater. 12 (2000) 2205.
[18] X.K. Li, Z.X. Lei, R.C. Ren, J. Liu, X.H. Zuo, Z.J. Dong, H.Z. Wang, J.B. Wang, Carbon 41 (2003) 3068.
[19] J.P. Cheng, X.B. Zhang, Z.Q. Luo, F. Liu, Y. Ye, W.Z. Yin, W. Liu, Y.X. Han, Mater, Chem. Phys. 95 (2006) 5.
[20] T.W. Ebbesen, H. Hiura, M.E. Bisher, M.M.J. Treacy, J.L. Shreeve-Keyer, R.C. Haushalter, Adv. Mater. 8 (1996) 155.
[21] R. Yu, L. Chen, Q. Liu, J. Lin, K. Tan, S. Choon Ng, H. Chan, G. Xu, T. Andy Hor, Chem. Mater. 10 (1998) 718.
[22] E. Dujardin, T.W. Ebbesen, H. Hirua, K. Tanigaki, Science 265 (1994) 1850.
[23] F.Z. Kong, X.B. Zhang, W.Q. Xiong, F. Liu, W.Z. Huang, Y.L. Sun, J.P. Tu, X.W. Chen, Surf. Coat. Technol. 155 (2002) 33.
[24] Y. Kotypin, A. Fernandez, T. Cristina Rojas, J. Campora, P. Palma, R. Prozorov, A. Gedanken, Chem. Mater. 11 (1999) 1331.
[25] S.K. Sharma, F.J. Vastola, P.L. Walker Jr., Carbon 35 (1997) 529.
[26] B.D. Cullity, Elements of X-ray Diffraction, Addison-Wesley, Reading, MA, 1978.
[27] J. Jiao, S. Seraphin, J. Phys. Chem. Solids 61 (2000) 1055.